# Simulation of Cold Roll Forming of Steel Panels

Fei-chin Jan
University of Pittsburgh
May 2000

# ABSTRACT

This project uses LS-DYNA to simulate the rolling deformation of a flat steel sheet into a panel of particular shape. The process involves the gradual deformation of the steel sheet by passing it through a series of rollers at a constant speed. Each of these sets of rollers is oriented at a slightly different angle to incrementally increase the deformation of the sheet until the desired geometry is obtained in the panel. Since the sheet could be going through several different sets of rollers at the same time, the deformation process is very complex and highly non-linear. During this process, the sheet metal panel undergoes plastic deformation and develops residual stresses. Some of the problems encountered with these panels include waviness surface, undesirable local deformation at the front (head) of the panel and excessive spring back of the end of the panel (tail). These problems are also observed in the results from the simulation and methods to minimize their effect are investigated. Other issues encountered in the simulation include the contact mechanism between the moving panel and a moving roller, effect of roller size and placement, panel thickness, panel speed and roller friction. An adaptive mesh was used to efficiently mesh the plate and rollers at critical locations. The results obtained should help improve both the simulation process and the actual cold-roll-forming-process especially when new or different metals are being introduced.

# INTRODUCTION

Cold forming processes are classified as brake forming or roll forming. Both processes are performed at room temperature with no heating of the material. In the brake forming process, the deformation of the whole panel is accomplished simultaneously in one step (see Figure 1-a), while in the cold roll forming process; the panel is gradually deformed using a piece-wise approach. The cross sections of roll formed panel will not be the same along the length of the panel during the rolling process (see Figure 1-b). A complex pattern of forming may produce considerable residual stresses on the panel (will be explained in the following). Some of the defects observed are shown in Figure 2. (Halmos, 1997)

The goal of this project is to simulate and analyze the cold roll forming process using LS-DYNA. The research is focused on investigating the wavy center formed after the cold rolling process by using explicit Finite Element Analysis (FEA) techniques. After the cold rolling process, a sheet metal panel has permanent deformation and residual stresses. Excessive defects make the panels unacceptable commercially to manufactures. The wavy effect is generated on the slope surface (as shown in Figure 3). The symmetric setting will be used in the roller setup simulation (as shown in Figure 3).

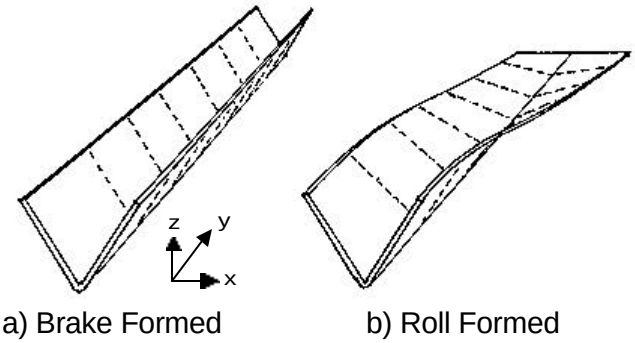


Figure 1 Cross Section Changes in Brake and Roll Formed "V" Section. (Halmos, 1997)

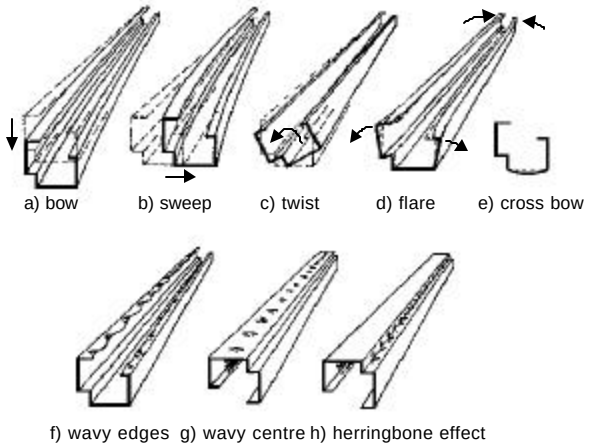


Figure 2 Undesirable effects found in cold roll form sections. (Halmos, 1997)

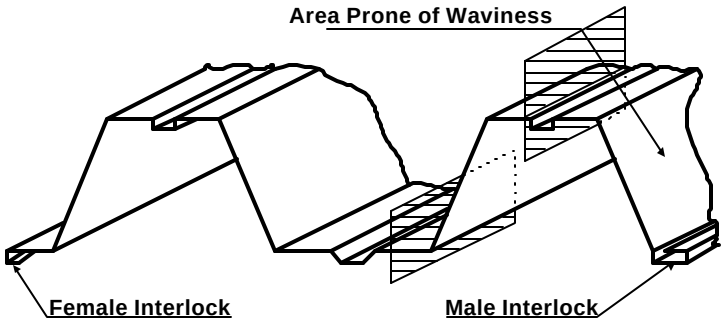


Figure 3 Typical cold roll form sections showing lines of symmetry.

## CHARACTERISTICS OF THE MODEL SETTING

1. Rollers are not rotating.
2. Rollers are modeled as rigid.
3. Rollers' surfaces are perfectly smooth.
4. The model is in a symmetric setting (as shown in Figure 3).
5. There is no rolling vibration considered.
6. Microstructures and mechanical properties of the plate are homogeneous.
7. The plate material is isotropic.
8. Applied displacement of bottom rollers to deform the plate.
9. Apply constant velocity on the plate—each node has a constant velocity in positive x-direction only.
10. The thickness of plate does not change after rolling deformation.
11. Belytschko-Tsay shell element is used on the plate and rollers. 5 integration points through the thickness is used on the plate.

# ROLLING SETTING AND PROCEDURE

The rolling setting is shown in Figure 4. The dimension of the plate is 1500×500×0.5mm. The diameter of main rollers is 300mm. The plate will be bended in 15 degrees as the shape of "Z." The center-to-center distance is 430mm.

The rolling procedure is listed in the following:

1. The plate is applied with a constant velocity in x-direction from the rest. As soon as the front end of the plate reaches the second set rollers, the bottom roller is applied with a displacement to deform the plate (as shown in Figure 5 and 6).
2. When the end of the plate leaves the first rollers set, the contact function is off. The plate is still going in x-direction (as shown in Figure 7).
3. As soon as the plate leaves the second rollers set, the contact function is off. Then, the data is collected alone the blue line (as shown in Figure 8).

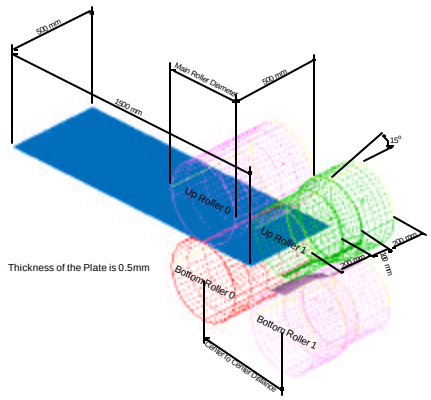


Figure 4 The model setup (bending radii are considered).

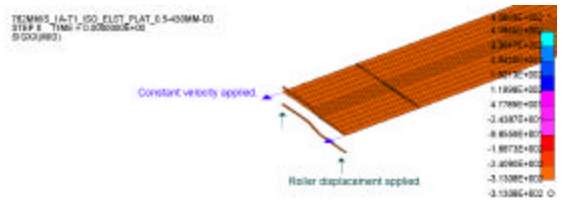


Figure 5 Step 1—before rolling deformation.

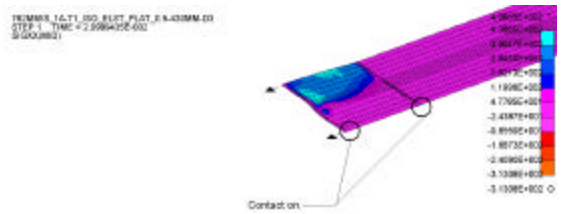


Figure 6 Step 2—the bottom roller deforms the plate.

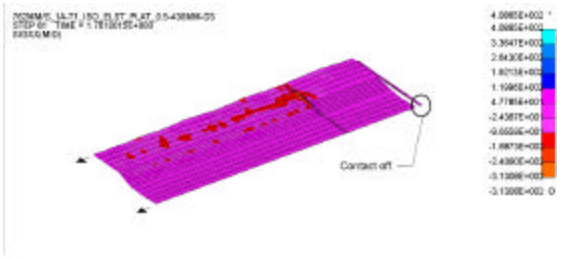


Figure 7 Step 3—the plate leaves the first set rollers.

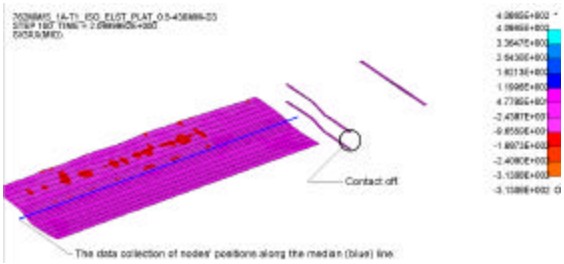


Figure 8 Step 4—the plate leaves the second set rollers.

## RESULTS

In Figure 9, the results are the comparison of applying different coefficients of friction (top/bottom plate) between the plate and rollers. This chart does not have tension applied on the plate during or after the rolling deformation. It can be best improved by applying the coefficients of friction in 0.05/0.1 and 0.1/0.05.

In Figure 10, the plate is applied with tension after rolling deformation. The tension stresses are greater than the plate's yield stress—365.9Mpa. Based on references, the waviness surface can be improved by applying tension stresses after cold-roll formed, but not in the simulation analysis.

In Figure 11, it is the comparison of the applied tension which is added on the plate during and after the rolling deformation with the best setting of coefficients of friction—0.1/0.05 and 0.05/0.1. No any result found in this respect yet, so more investigation is needed.

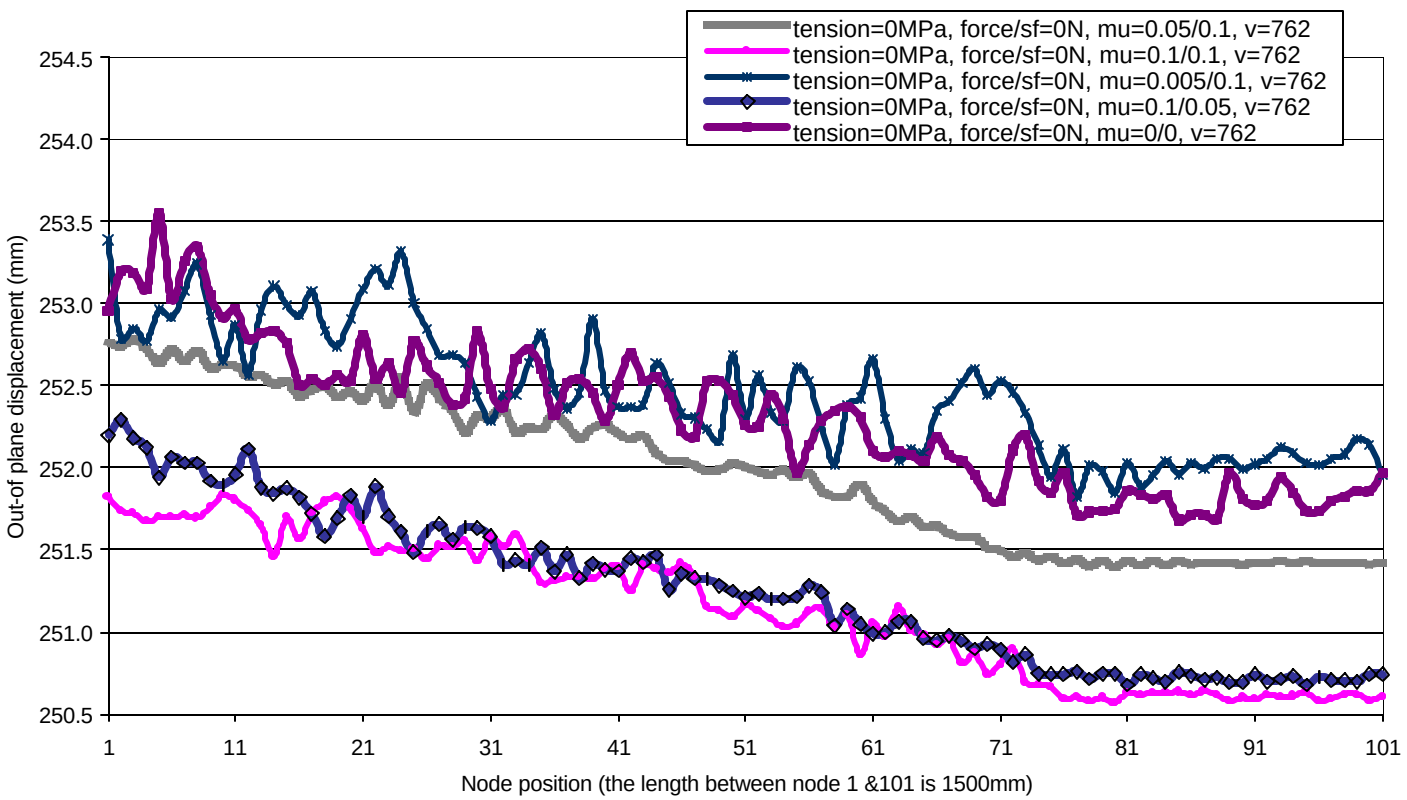


Figure 9 Rolling with friction

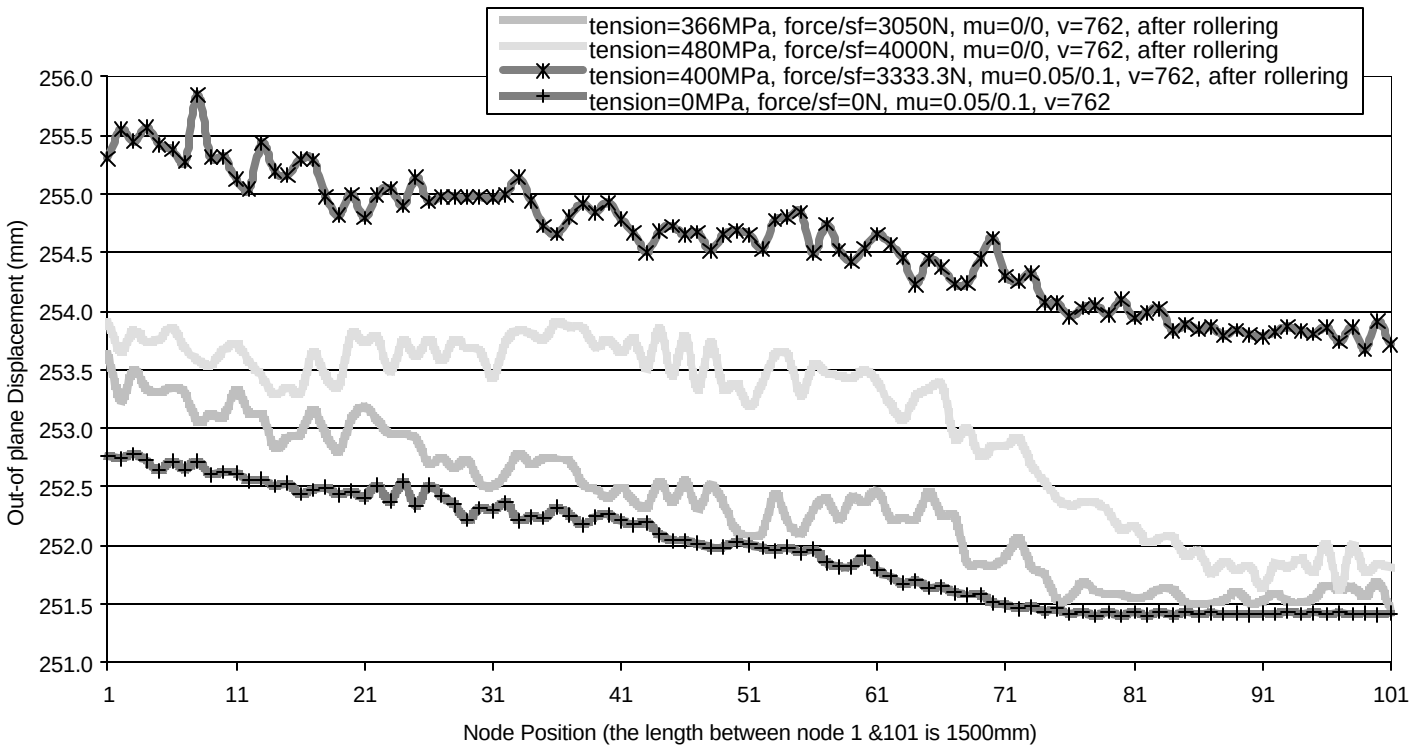


Figure 10 Tension applied on the plate after rolling

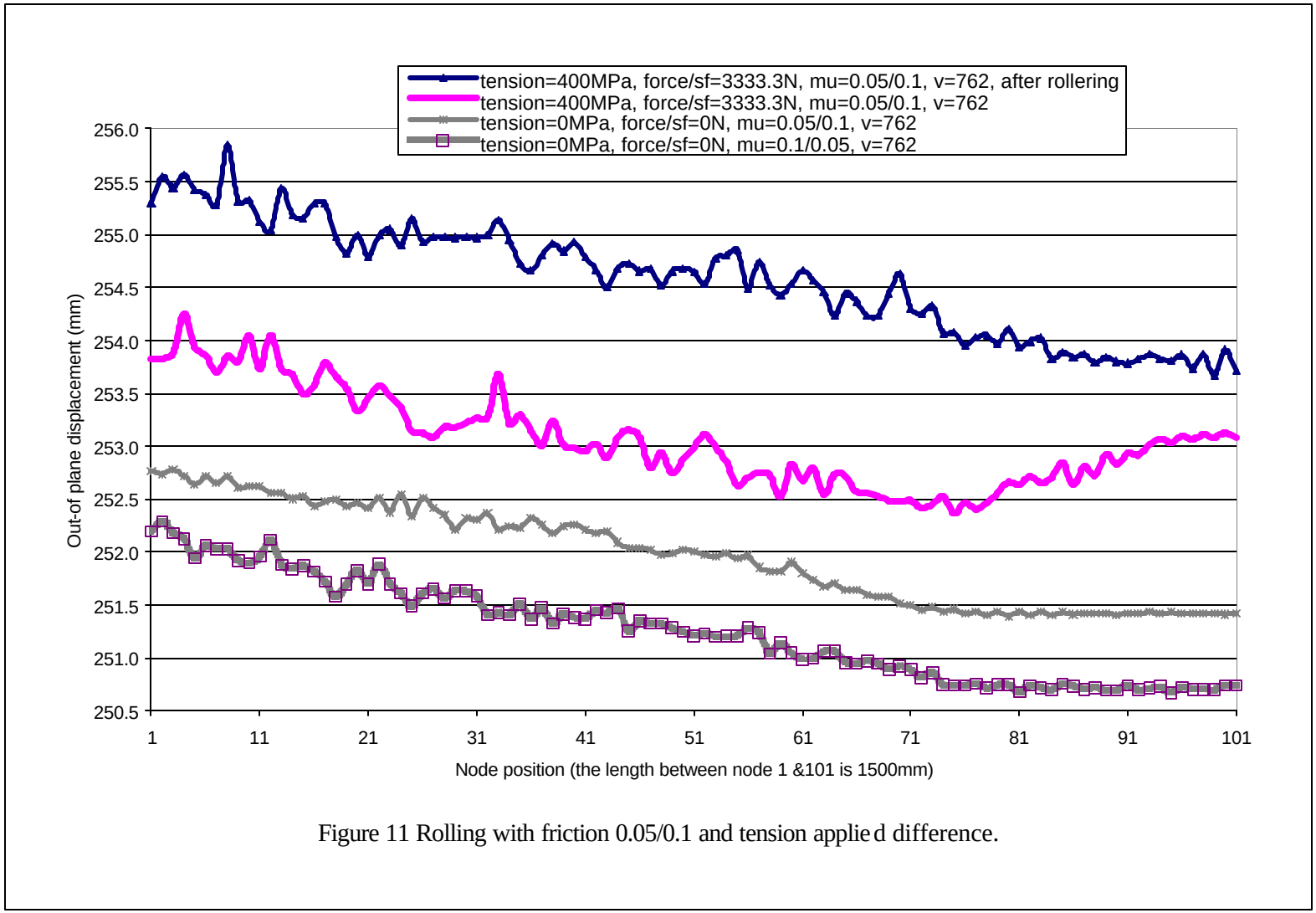


Figure 11 Rolling with friction 0.05/0.1 and tension applied difference.

## DISCUSSION OF RESULTS

This section is to explain the phenomenon of interaction between friction forces and waviness surface after the plate has been rolling deformed based on the results. A small element of the bending plate, as shown in Figure 12, will be analyzed by using the force and moment equilibrium. In order to investigate the interaction between the plate and rollers, the dynamic and rolling frictions are considered. Dynamic friction, tension, and normal force are mainly discussed in the simulation analysis.

Based on the definition of friction (as shown in equation 1), friction force only exists with normal force acting on an object (as shown in Figure 13). The interspace between rollers is the same as the thickness of plate as defined in the simulation, so friction force only occurs either on the top or bottom of the plate. And, friction force will not happen on the both sides of the plate simultaneously.

$$f_{dn} = m_{dn} N_{dn} \tag{1}$$

### *Dynamic Friction Analysis (Simulation)*

In the rolling simulation, rollers are fixed, so only dynamic friction occurs when the plate moves during the rolling deformation. The 3-D force equilibrium analysis is shown in Figure 14(a). All forces are indicated to act at the central gravity of the element. The thickness of the plate is the same as the interspace between two rollers as shown in Figure 13. To clearly express the force equilibrium analysis, the diagram is exaggeratedly demonstrated in Figure 14(a). During the rolling deformation, the plate is going to positive x-direction with velocity—v. The compression force, S, varies with the

element width, dw, and time, t. The angle, θ, is between the compression force and y-axis as shown in Figure 14(c). The sum of vertical components of compression force is considered as a normal force to act on the element. The tension, which varies with time t and along plate thickness, directs to the negative x-direction. The dynamic friction force is depending on $F_{ZZ}$. A force, which varies with time--t, is added to set force equilibrium directing to the positive x-direction. The side view of the force equilibrium analysis is shown in Figure 14(b). The $F_{ZZ}$ is the sum of the components of compression force, S, in z-direction, as shown the following:

$$F_{ZZ} = S\sin q + (S + \frac{\partial S}{\partial w} dw)\sin(q + \frac{\partial q}{\partial w} dw) \qquad (2)$$

In the simulation analysis, the element of plate has height $t_h$, length $dl$, and width dw. The two rollers are fixed as shown in Figure 15 and 16. In Figure 15, the bottom friction is generated by $F_{ZZ}$ and the weight of element $gdm$. The tension force directs to the negative x-direction. The plate has a constant velocity to the positive x-direction. So, "$F_{xx}$" has to be added and it directs to the positive x-direction because of the Newton third law. It is in the centerline of the element in the simulation analysis. $h_T$ indicates the height of the tension from the center of the element. The tension force is shown in Figure 15 and the following equation:

$$T = \int_0^{t_h} \mathbf{s} dt_h \qquad (3)$$

The sum of forces in the x and z directions are

$$\sum F_x = F_{XX} - T - f_{dn} = 0 \qquad (4)$$

$$\sum F_z = N_{dn} - gdm - F_{ZZ} = 0 \qquad (5)$$

The moment balance at point o is

$$\sum M_o = Th_T - f_{dn}\frac{t_h}{2} = 0 \tag{6}$$

When the sum of components of compression force $F_{ZZ} > gdm$ that acts upward, the upper friction force affects the plate movement as shown in Figure 16. The force and moment equilibrium are

$$\sum F_x = F_{XX} - T - f_{up} = 0 \tag{7}$$

$$\sum F_z = F_{ZZ} - N_{up} - gdm = 0 \tag{8}$$

$$\sum M_o = Th_T + f_{dn}\frac{t_h}{2} = 0 \tag{9}$$

### *Rolling Friction Analysis*

In the following discussion, we assume that the angular velocities of real rolling process are identical. In the diagram of real rolling process as shown in Figure 17, the second rolling set is applied $w_{up}$ and $w_{dn}$ that are equal as the above assumption, so the tangent velocities of surface ③ and ⑧ are the same as the velocity of the plate movement. Slip conditions occur between the plate and surface ④, ⑤, ⑥, and ⑦ as shown in Figure 17 and 18. The force $F_{XX}$ (as shown in Figure 19 and 20) is equal to the force that is generated by rollers. Three rolling circumstances between the plate and surface ⑤-⑧, ④-⑦, and ③-⑥, will be discussed separately.

When the plate is under rolling deformation by two sets of rollers, the applied force is shown in Figure 19. At the left end of plate, the force is evenly generated by the first set of rollers. At the right end of plate, the driven force acts seprately because

surface ③ and ⑧ draw the plate to the positive x-direction, and surface ④, ⑤, ⑥, and ⑦ slide on the plate (They will be discussed as follows).

**I.** Relation of the plate, and surface ⑤ and ⑧: The relation of tangential velocities of surface ⑤ and ⑧ is $w_{up} \times r_1 < w_{dn} \times r_2$ because $r_2 > r_1$ and $w_{up} = w_{dn}$ as shown in Figure 19 and 20. There is no slip status between the plate and bottom roller (surface ⑧), so the tangential velocity of bottom roller is equal to the plate velocity. Both rolling force $F_{XX}^*$ and compression force $F_{ZZ}$ vary with time t. The tension T varies with time t and thickness $t_h$. The element weight is $gdm$. When the compression $F_{ZZ} \le gdm$ as shown in Figure 19, the force and moment equilibrium are shown below:

$$\sum F_x = F_{XX}^* - T = 0 \tag{10}$$

$$\sum F_z = N_{dn} - F_{ZZ} - gdm = 0 \tag{11}$$

$$\sum M_o = F_{XX}^* \frac{t_h}{2} + Th_T = 0 \tag{12}$$

The dynamic friction force $f_{up}^*$ depends on $F_{ZZ}$. When the compression force $F_{ZZ} > gdm$ which acts upward as shown in Figure 20, the force and moment equilibriums are shown below:

$$\sum F_x = F_{XX}^* - f_{up}^* - T = 0 \tag{13}$$

$$\sum F_z = F_{ZZ} - N_{up} - gdm = 0 \tag{14}$$

$$\sum M_o = f_{up}^* \frac{t_h}{2} + Th_T + F_{XX}^* \frac{t_h}{2} = 0 \tag{15}$$

**II.** Relation of the plate, and surface ④ and ⑦: Both rollers are slipping with the plate because the two radii r are less than $r_2$, so the tangential velocities are less than the plate movement. The rolling force, directing to the right, varies with time t and location along the element thickness (as shown in Figure 21 and 22). When the compress force $F_{ZZ} \le gdm$ which acts downward as shown in Figure 21, the force and moment equilibrium are shown below:

$$\sum F_x = F_{XX}^* - f_{dn}^* - T = 0 \tag{16}$$

$$\sum F_z = N_{dn} - F_{ZZ}\cos f - gdm\cos f = 0 \tag{17}$$

$$\sum M_o = Th_T - f_{dn}^* \frac{t_h}{2} - F_{XX}h_F = 0 \tag{18}$$

When the compression force $F_{ZZ} > gdm$ which acts upward as shown in Figure 19, the force and moment equilibrium are shown below:

$$\sum F_x = F_{XX}^* - f_{up}^* - T = 0 \tag{19}$$

$$\sum F_z = F_{ZZ}\cos f - gdm\cos f - N_{up} = 0 \tag{20}$$

$$\sum M_o = Th_T + f_{up}^* \frac{t_h}{2} - F_{XX}h_F = 0 \tag{21}$$

**III.** Relation of the plate, and surface ③ and ⑥: The relation of tangential velocities of surface ③ and ⑥ is $w_{up} \times r_2 < w_{dn} \times r_1$ in Figure 23 and 24. There is no slip status between the plate and upper roller, so the tangential velocity of upper roller is the same as the plate velocity. When the compress force $F_{ZZ} > gdm$ as shown in Figure 23, the force and moment equilibrium are shown below:

$$\sum F_x = F_{XX}^* - T = 0 \tag{22}$$

$$\sum F_z = F_{ZZ} - N_{up} - gdm = 0 \tag{23}$$

$$\sum M_o = Th_T - F_{XX}^* \frac{t_h}{2} = 0 \tag{24}$$

When the compression force $F_{ZZ} \leq gdm$ which acts downward as shown in Figure 24, the force and moment equilibrium are shown below:

$$\sum F_x = F_{XX}^* - f_{dn}^* - T = 0 \tag{25}$$

$$\sum F_z = N_{dn} - F_{ZZ} - gdm = 0 \tag{26}$$

$$\sum M_o = Th_T - f_{dn}^* \frac{t_h}{2} - F_{XX} \frac{t_h}{2} = 0 \tag{27}$$

**Relation of Friction and Waviness of Rolling Deformed Plate**

The above discussion of the theoretical balances of force and moment is under perfect condition. Based on the results of the simulation, the relative coefficient of friction is the major factor of the waviness surface after rolling deformed plate. Let's use simple examples to describe the relation of friction and waviness surface of the deformed plate: The moment of friction force f(t), as shown in Figure 25 and 26, depends on the compression force that is changing with time, so the plot is a sinusoidal wave which respects to time in x-axis and moment of friction force in y-axis. The moment of the concentration of tension T(t), as shown in Figure 25 and 26, varies with time. The sinusoidal wave respects to time and the moment of tension. The sum of moments of friction and tension waves is W(t) which is the waviness surface after rolling deformed.

If f(t) and T(t) are close to 90$^{o}$ out of phase, the amplitude of W(t) will be reduced.

Otherwise the amplitude of W(t) will be increased.

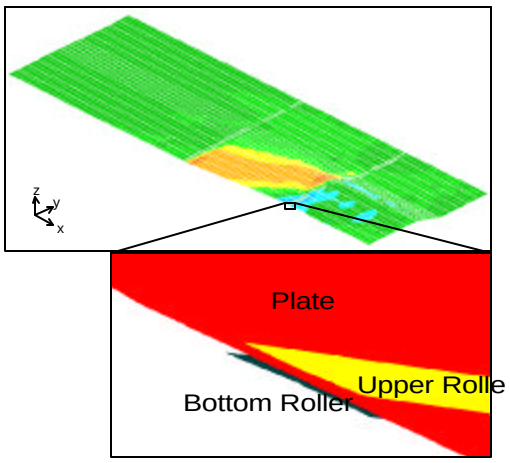


Figure 12 Zoom-in of the element of plate analysis.

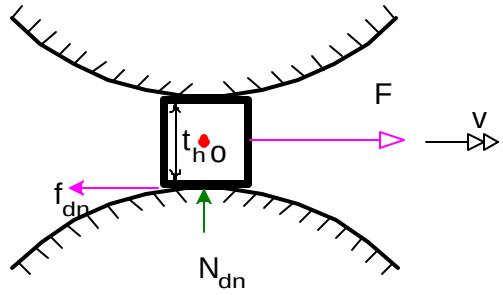


Figure 13 Free-body diagram of a friction force and a force act on an element of rolling simulation.

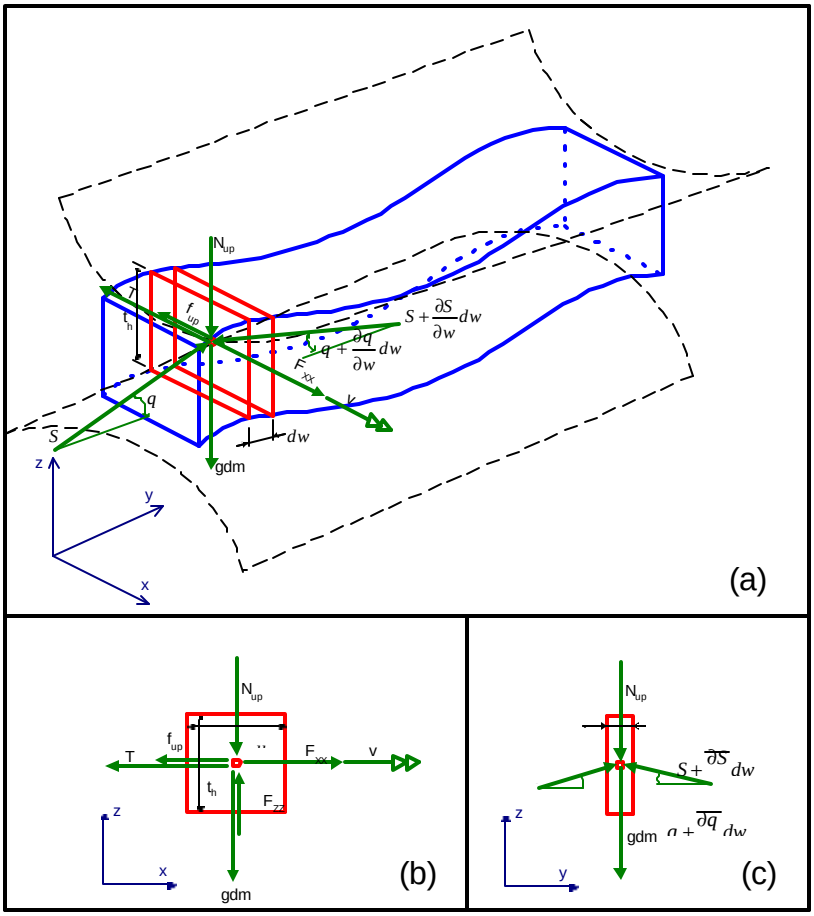


Figure 14 Three dimension free-body diagram of the element analysis.

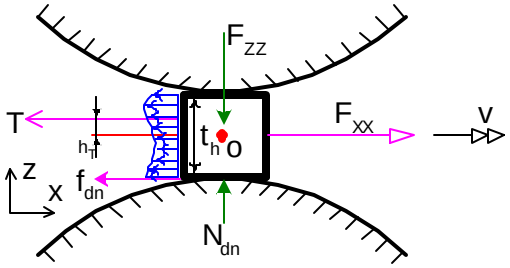


Figure 15 Free-body diagram of the bottom friction force and tension act on an element of the plate in the simulation.

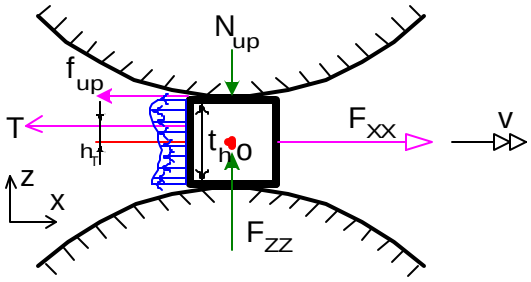


Figure 16 Free-body diagram of the upper friction force and tension act on an element of the plate in the simulation.

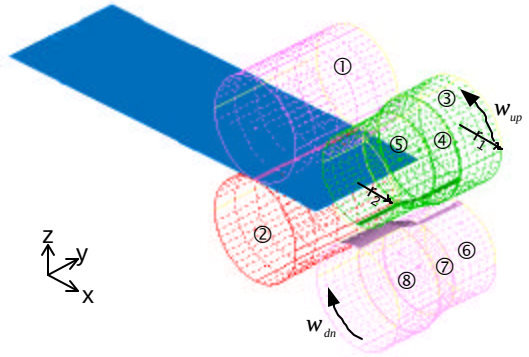


Figure 17 The iso-view of real rolling diagram.

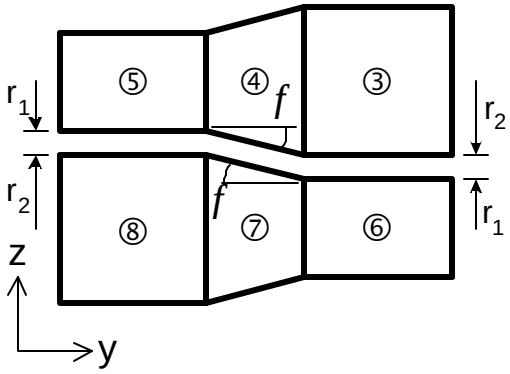


Figure 18 The front view of second set of rollers.

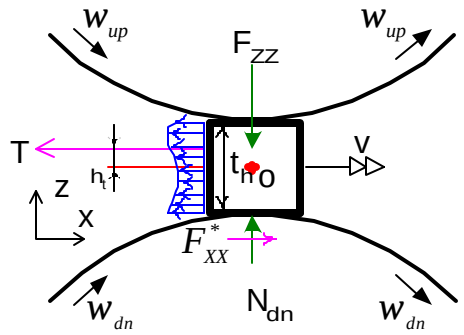


Figure 19 Analysis of real rolling at surface ⑤ and ⑧.

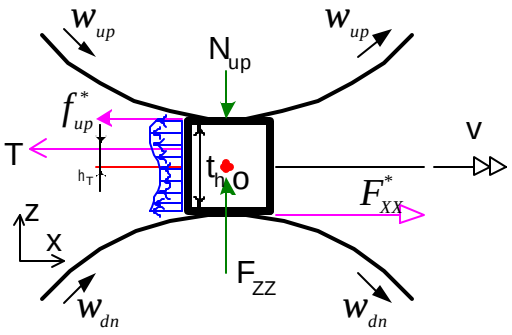


Figure 20 Analysis of real rolling at surface ⑤ and ⑧.

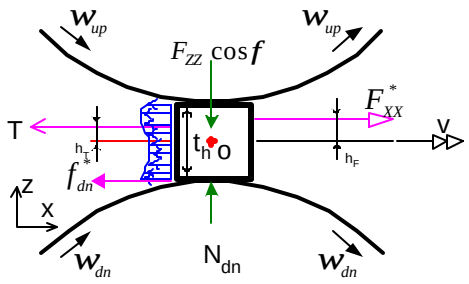


Figure 21 Analysis of real rolling at surface ④ and ⑦.

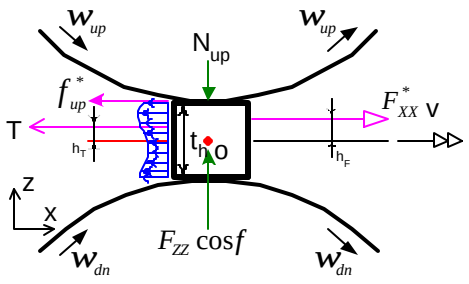


Figure 22 Analysis of real rolling at surface ④ and ⑦.

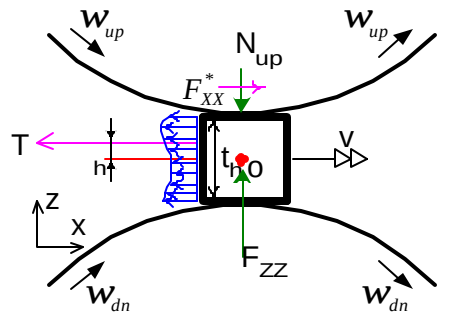


Figure 23 Analysis of real rolling at surface ③ and ⑥.

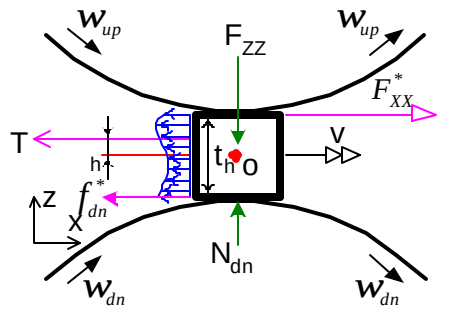


Figure 24 Analysis of real rolling at surface ③ and ⑥.

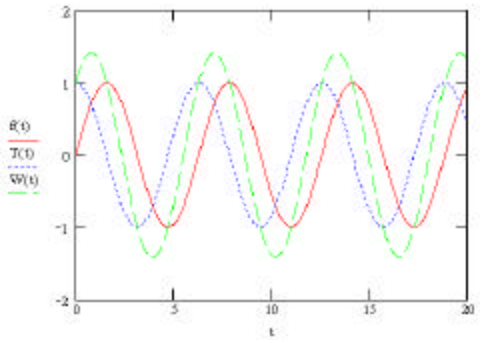


Figure 25 Response of friction, tension, and the sum of friction and tension.

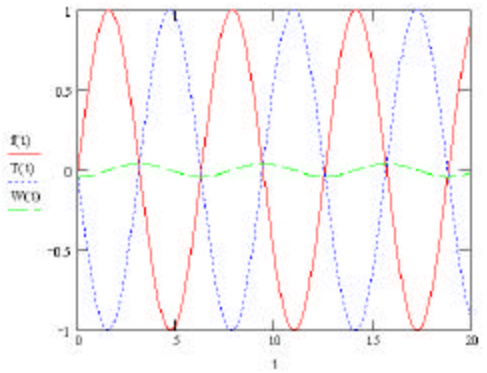


Figure 26 Response of friction, tension, and the sum of friction and tension.

## CONCLUSION & FUTURE WORK

As references have shown, the applied tension will improve the waviness of the plate surface, however, it is not so in the findings of my simulation. This means that more investigation into this aspect is needed. Moreover, the measurements of the ratios of coefficient friction needs to be done.

For future work, springback and bending radii measurements need to be considered as well. Based on the discussion of results, solid element should be applied on the plate and the rollers should be set rotating for more advanced analysis.

## REFERENCE


Altan, T., Gegel, H. L., & Oh, S. I. (1983). Metal Forming: Fundamentals and Applications. Metals Park, OH: Carnes Publication Services, Inc.

Altan, T., Kobayashi, S., & Oh, S. I. (1989). Metal Forming and the Finite-Element Method. New York, NY: Oxford University Press.

Bauld, N.R. (1986). Mechanics of Materials. Boston, MA: PWS Publishers. P632.

Baxter, H. L. & Betts, W. H. (1990). Rolls Used in Today's Rolling Mills-- Rolls for the Metalworking Industries. A Publication of the Iron and Steel Society, Inc.: Warrendale, PA. (p23-p30)

Caddell, R. M. & Hosfort, W. F. (1993). Metal Forming Mechanics and Metallurgy. Englewood Cliff, NJ: Prentice-Hall, Inc.

Chaudhry, S., Wang, S.P., & Wertheimer, T.B. Comparison between the static implicit and dynamic explicit methods for FEM simulation of sheet forming processes. http://www.marc.com.

Chen, W. & Saleeb, A. F. (1994). Constitutive Equations for Engineering Materials (Volume 1). New York, NY: Elsevier Science B.V. (p150-p157)

Dobrev, A. & Halmos, G. T. Roll Design. Charlotte, NC: FMA's Roll Forming Conference 1997.

Dong, C. (1998). Deformation Mechanics in Cold-Roll-Formed Wide Profiles. M. S. Project. University of Pittsburgh.

Donmez, O. E. (1997). Inelastic Deformation of Metals Using Finite Element Method. M. S. Project. University of Pittsburgh.

Dowing, N. E. (1993). Mechanical Behavior of Materials. Upper Saddle River, New Jersey: Prentice-Hall, Inc. (p148-p150)

Eibe, W. W. (1990). History of the Development of Rolling Mills and Their Rolls—Rolls for the Metalworking Industries. A Publication of the Iron and Steel Society, Inc.: Warrendale, PA. (p1-p22)

Halmos, G. T. (1997). Roll Forming HSLA Steels. Charlotte, NC: FMA's Roll Forming Conference 1997.

Halmos, G. T. (1997). Roll Forming to Tight Tolerances. Charlotte, NC: FMA's Roll Forming Conference 1997.

Halmos, G. T. (1997). Selecting the Right Material for Roll Forming and Brake Forming. Charlotte, NC: FMA's Roll Forming Conference 1997.

Hira, T., Abe, H. & Nakagawa, K. (1979). Effect of the Mechanical Properties of Steel Sheet on Web-Buckling Behavior in the Cold Roll-Forming of Sliding Board. Journal of the Japanese Society of Technology and Plasticity, Vol. 20, No. 225 pp. 933-939.

Miyamato, Y. & Hawa, S. (1991). Effect of Tensile Flow Properties of Titanium Sheets on web-Buckling Behavior in Cold Roll-Forming of Wide Profiles. ISIJ International, Vol. 31 No. 8, pp. 863-869.

Ona, H. & Jimma, T. (1994). Prevention of Shape Defects in the Cold-Roll Forming Process of Wide Profiles. Bulletin of Precision Machinery and Electronics, Tokyo Institute of Technology, No. 53, pp. 1-13.

Roberts, W. L. (1978). Cold Rolling of Steel. New York, NY: Marcel Dekker, Inc.
Taylor, R. L. & Zienkiewicz, O. C. (1988). The Finite Element Method ($4^{th}$ ed). Lodon, UK: McGraw-Hill Book Company.

Roberts, W. L. (1990). The Rolling Process Mechanical Engineering Explanation—Rolls for the Metalworking Industries. A Publication of the Iron and Steel Society, Inc.: Warrendale, PA. (p31-p54)

Schuler GmbH (1998). Metal Forming Handbook. Berling, Germany: Springer-Verlag. (p373-p388)

Wang, C. T. (1993). Mechanics of Bending, Flanging, and Deep Drawing and a Computer-Aided Modeling System for Predictions of Strain, Fracture, Wrinkling and Springback in Sheet Metal Forming. Ph.D Dissertation. Ohio State University.

Wu, H. C. (1999). Analytical and Numerical Investigation of Sheet Metal Bending, Flanging and Hemming. M.S. Thesis. Ohio State University.